THE JOURNAL OF BIOLOGICAL CHEMISTRY
Vol. 278, No. 4, Issue of January 24, pp. 2630–2635, 2003

Printed in U.S.A.

Structural Consequences of a Cancer-causing BRCA1-BRCT Missense Mutation*

Received for publication, September 30, 2002, and in revised form, October 23, 2002
Published, JBC Papers in Press, November 8, 2002, DOI 10.1074/jbc.M210019200

R. Scott Williams and J. N. Mark Glover‡

From the Department of Biochemistry, 437 Medical Sciences Building, University of Alberta, Edmonton T6G 2H7, Canada

The integrity of the carboxyl-terminal BRCT repeat region is critical for BRCA1 tumor suppressor function; however, the molecular details of how a number of clinically derived BRCT missense mutations affect BRCA1 function remain largely unknown. Here we assess the structural response of the BRCT tandem repeat domain to a well characterized, cancer-associated single amino acid substitution, Met-1775 → Arg-1775. The structure of BRCT-M1775R reveals that the mutated side chain is extruded from the protein hydrophobic core, thereby altering the protein surface. Charge-charge repulsion, rearrangement of the hydrophobic core, and disruption of the native hydrogen bonding network at the interface between the two BRCT repeats contribute to the conformational instability of BRCT-M1775R. Destabilization and global unfolding of the mutated BRCT domain at physiological temperatures explain the pleiotropic molecular and genetic defects associated with the BRCA1-M1775R protein.

Germ line mutations within the breast and ovarian cancer susceptibility gene *BRCA1* predispose carriers to early onset breast and ovarian cancer, and it is estimated that ~5–10% of all breast cancers are caused by inheritance of dominant disease genes (1). Various lines of evidence suggest that the BRCA1 protein product is involved in the regulation of multiple nuclear functions including transcription, recombination, DNA repair, and checkpoint control (for reviews, see Refs. 2–4). BRCA1 is an 1863-amino acid nuclear phosphoprotein that includes an amino-terminal RING finger domain and two tandem carboxyl-terminal repeats, termed the BRCT domain. The importance of the conserved RING and BRCT domains to the tumor suppressor function of BRCA1 is demonstrated by the fact that the majority of known cancer-causing BRCA1 mutations localize to these domains (5–9).

The extreme carboxyl-terminal region of BRCA1 contains two ~90–100 amino acid sequence repeats called BRCT[1] (**BR**CA1 **c**arboxyl-**t**erminal) repeats that are the prototypical members of a protein fold superfamily that includes many proteins associated with DNA repair (10–12). The recently determined x-ray crystal structures of the human (13) and rat (14) BRCA1 BRCT repeats provide a framework for the interpretation of BRCT mutations identified in patients from breast cancer screening programs. The two structurally similar BRCT repeats resemble the structures of the isolated BRCT domains from XRCC1 (15) and DNA ligase III (16) and are composed of a central four-stranded, parallel β-sheet flanked by a single α-helix on one side (α2), with a pair of α-helices (α1 and α3) and a short 3_{10}-helix on the opposite side. The two repeats are connected by a relatively flexible linker and pack together in a specific, head-to-tail manner that is conserved not only between human and rat BRCA1 but also in the BRCT domain of the p53-interacting protein, 53BP1 (13, 14).

Several cancer-associated BRCT missense mutations (1, 6) have been characterized in functional detail. Two extensively studied variants, A1708E and M1775R, ablate double-strand break repair and transcription function of BRCA1 (17–19) and inhibit BRCT interactions with histone deacetylases (20), the DNA helicase BACH1 (21), and the transcriptional co-repressor CtIP (22, 23). Both of these mutations occur at the interface between the amino- and carboxyl-terminal BRCT repeats and are predicted to affect the way in which the two repeats interact. The enhanced sensitivity of the A1708E mutant to proteolytic digestion indicates that this mutation has profound structural consequences (13). In contrast, the M1775R mutant displays a proteolytic sensitivity that is intermediate between that of the wild type protein and the A1708E mutant, suggesting that the M1775R mutation results in a milder structural defect.

In the present study we employed limited proteolysis, CD spectroscopy, and x-ray structural analysis to probe the structural consequences of the M1775R mutation. Our results show that the methionine-arginine substitution leads to a rearrangement of the BRCT repeat interface, alterations in the surface of the protein, and global destabilization of the BRCT domain.

EXPERIMENTAL PROCEDURES

Proteolysis—For proteolytic assays, BRCT-WT and BRCT-M1775R were expressed from the T7 expression vector pLM1 and labeled with [^{35}S]methionine using the TNT-Quick *in vitro* transcription/translation system (Promega). Immediately before digestion, proteins were translated at 30 °C for 2 h. The reticulocyte lysates were then centrifuged for 2 min at 10000 × *g* to remove insoluble material; 3 μl of the lysate supernatants containing the labeled translation products were added to 12 μl of digestion buffer (150 mM NaCl, 50 mM potassium phosphate, pH

* This work was supported by funding from the Canadian Breast Cancer Research Initiative, the Canadian Institutes of Health Research, the National Cancer Institute of Canada, and the Alberta Heritage Foundation for Medical Research. Use of the Argonne National Laboratory Structural Biology Center beamlines at the Advanced Photon Source was supported by the U. S. Department of Energy, Office of Biological and Environmental Research under Contract No. W-31–109-ENG-38. The costs of publication of this article were defrayed in part by the payment of page charges. This article must therefore be hereby marked "*advertisement*" in accordance with 18 U.S.C. Section 1734 solely to indicate this fact.

The atomic coordinates and structure factors (code 1N5O) have been deposited in the Protein Data Bank, Research Collaboratory for Structural Bioinformatics, Rutgers University, New Brunswick, NJ (http://www.rcsb.org/).

‡ To whom correspondence should be addressed. Tel.: 1-780-492-2136; Fax: 1-780-492-0886; E-mail: mark.glover@ualberta.ca.

[1] The abbreviations used are: BRCT, BRCA1 carboxyl-terminal domain; CTIP, CtBP interacting protein; MES, 4-morpholineethanesulfonic acid.

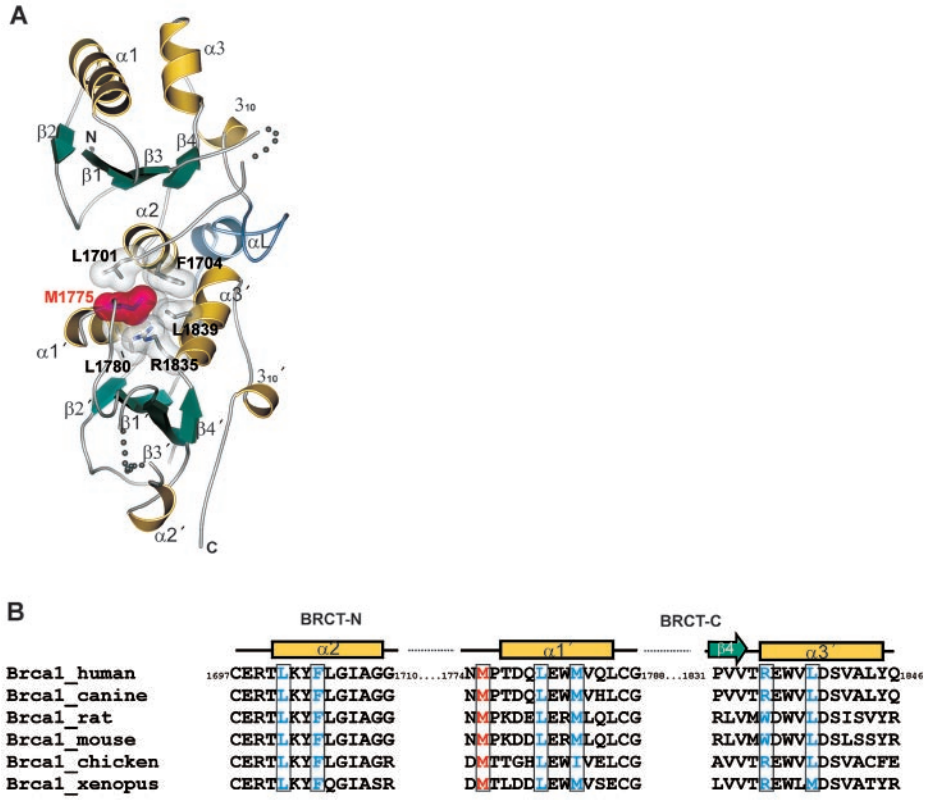

FIG. 1. **Evolutionary conservation of the Met-1775 packing environment.** *A*, ribbons diagram of the BRCT repeat region of BRCA1. Met-1775 (*red*) in BRCT-WT is positioned between the two BRCT fold repeats. Met-1775 (*red surface*) lies in a hydrophobic pocket created by Leu-1701, Phe-1704, Leu-1780, Met-1783 (behind Met-1775), Arg-1835, and Leu-1839 (*gray surfaces*). *B*, multiple sequence alignment of BRCA1 homologues for the BRCT regions surrounding Met-1775. Met-1775 is *red*, and contacting amino acids are *blue*. Numbering is for human BRCA1.

7.5) containing increasing concentrations of 1-chloro-3-tosylamido-7-amino-2-heptanone (TLCK)-treated chymotrypsin (Sigma). Following digestion at 20 or 37 °C for 12 min, the reactions were stopped with phenylmethylsulfonyl fluoride. Digestion products were electrophoresed on 15% SDS-PAGE gels and visualized with a phosphorimaging plate and an Amersham Biosciences Typhoon scanner. Quantification of the reaction products within ImageQuant (Amersham Biosciences) used a local average background correction.

Protein Expression and Purification—Expression and purification of recombinant human BRCA1-(1646–1859) (BRCT-WT) and BRCA1-(1646–1859)-M1775R (BRCT-M1775R) was performed essentially as described (13), with some changes. When expressed at 30 and 37 °C, yields of BRCT-M1775R were greatly reduced relative to BRCT-WT, likely because of degradation. To obtain large quantities of BRCT-M1775R protein for crystallization studies, growth of cells and induction of protein expression were carried out at 25 °C. Purification using a combination of ammonium sulfate precipitation, hydrophobic interaction, gel filtration, and anion exchange chromatography yielded 4–5 mg of protein/liter *Escherichia coli* culture for both proteins. Matrix-assisted laser desorption ionization time-of-flight (MALDI-TOF) mass spectrometric analysis confirmed mutation of residue Met-1775 to arginine.

CD Spectroscopy—For circular dichroism measurements, proteins were dialyzed into 400 mM NaCl, 50 mM potassium phosphate (pH 7.5), 0.1% β-mercaptoethanol, in a Millipore Ultrafree-10 concentration unit. Protein concentrations for molar ellipticity calculations were derived from amino acid analysis. Far-UV (195–255 nm) CD spectra were determined using 0.2 mg/ml solutions of protein and were acquired using a Jasco J-720 spectrapolarimeter that was interfaced with Jasco software and equipped with a 0.1-cm quartz cuvette cell. For denaturation experiments, temperature within the cell was regulated using a Peltier thermal control unit. Assuming a two-state unfolding model, denaturation midpoints were determined by following the change in molar ellipticity at 222 nm as a function of temperature. Measurements were taken at 0.5 °C intervals, and the temperature was increased at a rate of 30 °C/h. Ellipticity readings were normalized to the mole fraction of protein folded (f_f) or denatured (f_u) using the standard equations

$$f_f = ([\theta] - [\theta]_u)/(([\theta]_n - [\theta]_u) \quad \text{(Eq. 1)}$$

$$f_u = (1 - f_f)$$

where $[\theta]_n$ and $[\theta]_u$ are the molar ellipticity for the fully folded and fully denatured protein species. $[\theta]$ is the observed ellipticity at each temperature. The midpoint of the temperature-dependent folding-unfolding transition for both proteins was reproducible, but this transition was irreversible and characterized by precipitation within the cell under the conditions used.

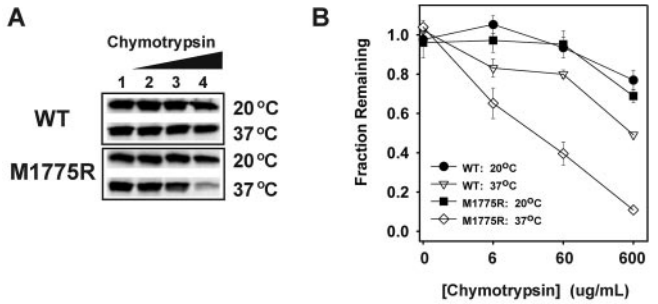

FIG. 2. **Protease sensitivity of BRCT-M1775R.** *A*, reticulocyte lysates containing ^{35}S-labeled, *in vitro*-translated BRCT-WT and BRCT-M1775R were digested at the indicated temperatures for 12 min using chymotrypsin at concentrations of 0, 6, 60, 600 μg/ml (*lanes 1–4*). Reaction products were analyzed by SDS-PAGE and autoradiography. *B*, quantification of chymotryptic digestions. The fraction remaining is the percent of starting protein present following digestion with the indicated concentrations of chymotrypsin. Data points are the mean value of digestions performed in triplicate with *error bars* reflecting the S.D.

Crystallization of BRCT-M1775R—Protein concentrations for crystallization were determined using the BCA protein assay (Pierce). Unlike the wild type protein, storage of the mutant at concentrations greater than 5 mg/ml resulted in irreversible aggregation within days. To attain high protein concentrations suitable for crystallization, BRCT-M1775R at 1 mg/ml was dialyzed into Protein buffer (400 mM NaCl, 5 mM Tris-HCl, pH 7.5) and concentrated to 20 mg/ml immediately prior to crystallization. Crystals were grown at room temperature (20–22 °C) using the hanging drop vapor diffusion technique. 2 μl of 20 mg/ml BRCT-M1775R in Protein buffer was mixed with 2 μl of well solution (1.4 M ammonium sulfate, 100 mM MES, pH 6.7, 10 mM $CoCl_2$) to produce hexagonal crystals within 1 to 2 days (see Table I).

Data Collection, Structure Solution, and Refinement—For data collection, crystals were gradually transferred to a cryoprotectant solution

containing 1.2 M ammonium sulfate, 100 mM MES, pH 6.7, 10 mM $CoCl_2$, 26% glycerol over the course of 45–60 min. Diffraction data to 2.8 Å resolution were collected from a single crystal at 100 K at the Structural Biology Centre (Argonne National Laboratory)-APS beamline 19-ID. Intensity data were processed using the HKL2000 package (24) (see Table I). Crystallographic phase information for BRCT-M1775R was obtained using molecular replacement with the native human BRCT model (RCSB, 1JNX) (13). All data between 20 and 2.8 Å were used in crystallographic refinement, and 7% of this data was allocated for cross-validation. Initial rigid body fitting of the model in the Crystallography and NMR System (CNS) (25) lowered the R_{factor}/R_{free} to 36.2/38.6%. Side chains of regions of the protein that change with mutation of the BRCT were built using O (26) into σ-A weighted model-phased F_o-F_c and $2F_o-F_c$ electron density maps calculated with CNS. Maximum likelihood targets, bulk solvent correction, and overall anisotropic B-factor scaling were applied throughout the refinement process. Further refinement involved iterative cycles of manual building and restrained refinement with translation, libration, and screw rotation group anisotropic thermal parameter modeling as implemented in REFMAC (v5.0.32) (27, 28). The quality of the model was assessed using PROCHECK (Ref. 29, Table I). The final model (see Table I) has good stereochemistry and a working R-factor of 27.3% (R_{free}, 29.8%) for all data in the resolution range 20–2.8 Å. Structural diagrams were created using BOBSCRIPT (30) and rendered with POVRAY (www.povray.org) (Figs. 1, 4, and 5, *A* and *B*) or RASTER3D (31) (Fig. 5, *C–E*). Molecular surfaces were drawn with GRASP (32).

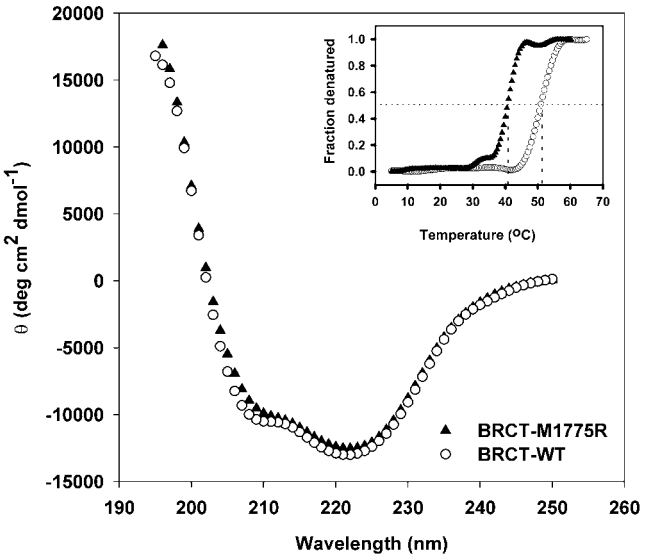

FIG. 3. **CD spectra.** The far-UV CD spectra for the wild type (○) and mutant protein (▲) are similar at 20 °C. Thermal denaturation of BRCT-WT and BRCT-M1775R. Molar ellipticity at 222 nm was measured, and the values were used to calculate a mole fraction of denatured molecules for each temperature (*inset*). Midpoints of the transitions (WT, 52 °C; M1775R, 41 °C) are marked by *dotted lines*.

RESULTS AND DISCUSSION

Native Packing Environment of Met-1775—The tandem BRCT repeat structure is composed of two α/β-fold BRCT domains that interact end-to-end, with helices $\alpha1'$ and $\alpha3'$ from the carboxyl-terminal BRCT intimately contacting $\alpha2$ from the amino-terminal repeat in a three-helix bundle-like packing arrangement (Fig. 1*A*) (13, 14). Residue Met-1775 is largely buried within the interface between the two repeats and lies in a pocket formed by Leu-1701 and Phe-1704 from the amino-terminal repeat and Leu-1780, Met-1783, Arg-1835, and Leu-1839 from the carboxyl-terminal repeat. Sequence and structural conservation of Met-1775 and its contacting residues among mammalian, xenopus, and avian BRCA1 homologues highlights the importance of Met-1775 in orienting the two BRCT repeats (Fig. 1*B*) (13, 14). With the exception of residue Arg-1835, which is replaced by a tryptophan in the mouse and rat BRCT domains, the residues forming this pocket are highly conserved. This substitution within the pocket is significant, however, as proximity of the positively charged residue Arg-1835 to Met-1775 in the human protein influences the response of the structure to the

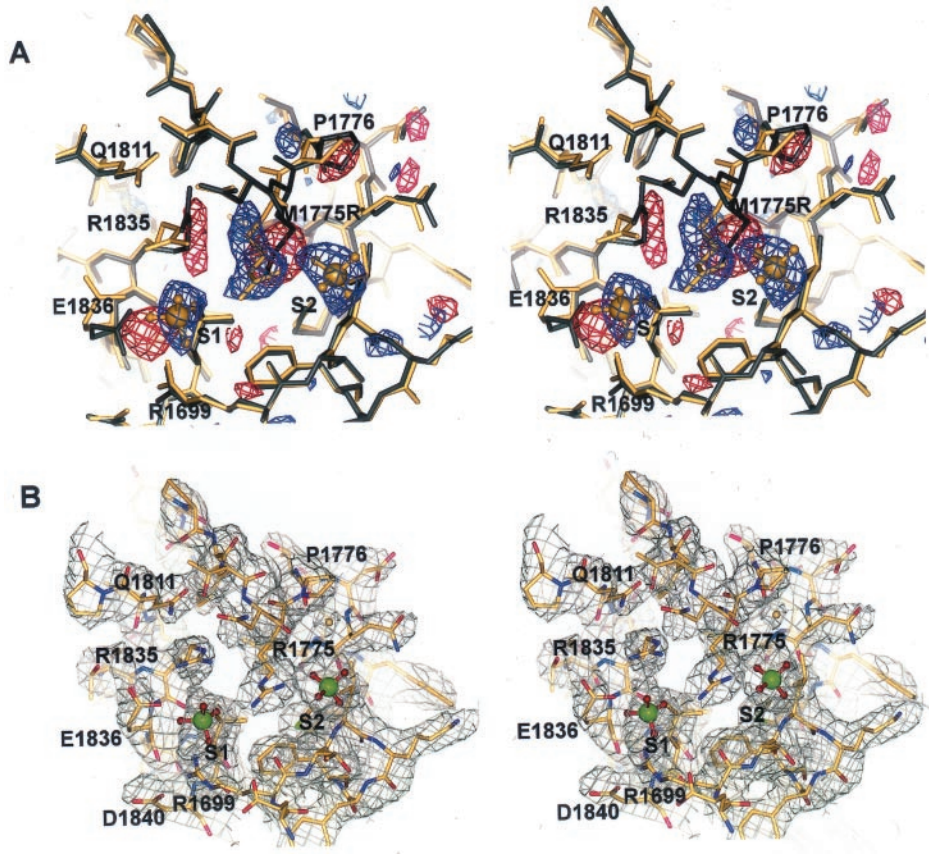

FIG. 4. **M1775R structure determination.** *A*, stereoview of an overlay of BRCT-WT (*gray*) and BRCT-M1775R (*gold*) for the region surrounding M1775R. The 2.8 Å positive (*blue*) and negative (*red*) σ-A weighted F_o-F_c electron density (phased with the wild type model, RCSB, 1JNX) is contoured at ± 2.9 σ. Two large positive peaks, modeled as sulfate molecules S1 and S2, are found coplanar to Arg-1775. *B*, a stereoview of model phased σ-A weighted 2 F_o-F_c map contoured at 1.0 σ is displayed for the final model of BRCT-M1775R. Electron density maps were calculated with CNS *(A)* or REFMAC *(B)*.

cancer-linked substitution, M1775R.

Proteolytic Sensitivity of M1775R—Mutant M1775R conferred moderate sensitivity to digestion with trypsin at 20 °C (13). Because Arg-1775 immediately precedes a proline residue, this substitution is not expected to introduce a new trypsin cleavage site; thus the enhanced trypsin sensitivity is an indication of a subtle structural change in the M1775R mutant. To further assess the stability of the M1775R mutant, we compared its chymotrypsin sensitivity to that of the wild-type protein (Fig. 2, *A* and *B*). BRCT-WT and BRCT-M1775R both show resistance to digestion at 20 °C for all protease concentrations. Elevating the temperature to 37 °C enhanced cleavage of the mutant by chymotrypsin at all protease concentrations, whereas the wild type showed only a slight increase in cleavage efficiency at the highest concentration. The fact that the BRCT-M1775R exhibits modest but significant increases in sensitivity to digestion by two proteases with different cleavage specificities, especially at elevated temperatures, indicates that M1775R results in a folding defect in the BRCT domain.

CD Analysis—To further probe the extent of protein destabilization induced by the M1775R substitution, we compared the secondary structure and thermal stability of BRCT-M1775R to the wild type protein using CD spectroscopy (Fig.

TABLE I
Crystallographic data and refinement statistics

Unit cell (space group $p6_122$) $a = b$ (Å)	114.708
c (Å)	121.676
Resolution range (Å)	50–2.8
No. of observed reflections	100,697
No. of unique reflections	12,024
Completeness (%)	99.3 (100)[a]
R_{sym} (%)[b]	6.8 (40.4)
Overall $I/\sigma I$	29.9 (3.3)
R_{cryst}/R_{free} (%)[c]	27.3/29.8
No. of residues/H_2O/SO_4^{2-}/Co^{2+}	213/59/2/1
Ramachandran plot (%):	
Most favored/allowed/generous/disallowed	87.2/11.7/1.1/0
RMSD bonds (Å)/angles (°)	0.013/1.857

[a] Values in parentheses are statistics for the highest resolution shell (2.90 − 2.80 Å).
[b] $R_{sym} = 100\ \Sigma_{hkl}|\langle I\rangle - I|/\Sigma_n\langle I\rangle$.
[c] $R_{cryst} = \Sigma_n|F_o(h) - F_c(h)|/\Sigma_n|F_o(h)|$, where $F_o(h)$ and $F_c(h)$ are observed and calculated structure factors for the resolution range 20–2.8 Å. R_{free} calculated with 7% of all reflections excluded from refinement.

TABLE II
Defects associated with BRCA1-M1775R

Deleterious effect	References
Mutant BRCA1 allele encoding BRCA1-M1775R segregates with disease in families with breast and ovarian cancer	1, 6
Impaired kinetics of double strand DNA break repair	17
Transcription activation activity abolished	18, 19
Impaired protein binding to CtIP	23
Impaired protein binding to histone deacetylase complexes	20
Impaired protein binding to the BACH1 DNA helicase	21

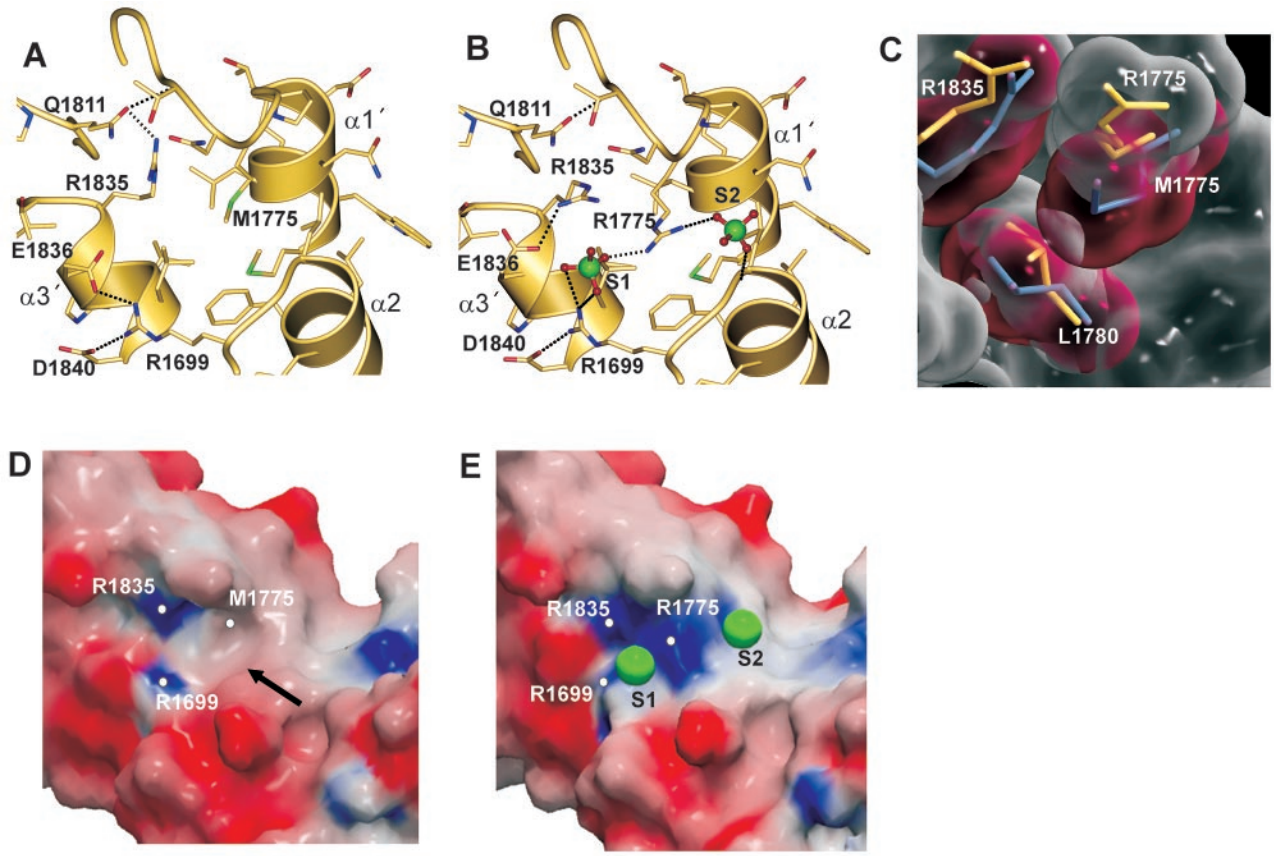

FIG. 5. **Structural rearrangements accommodate M1775R.** *A*, native hydrogen bonding interactions proximal to Met-1775. Hydrogen bonds are indicated by *dashed lines*. *B*, hydrogen bonding, salt bridging for mutant M1775R. Arg-1775 participates in the coordination of two solvent anions, S1 and S2, and has been flipped out from the hydrophobic pocket where Met-1775 normally packs. *C*, cutaway view of the hydrophobic core of the BRCT. Structural overlay of WT (*gray with red surface*) and M1775R (*gold with gray surface*) hydrophobic core residues that move upon mutation. *D*, charge potential GRASP surface for BRCT-WT. *Blue* surface reflects positive charge potential, and *red* is negative. The *arrow* indicates a hydrophobic groove near Met-1775. *E*, charge potential GRASP surface for BRCT-M1775R. *Green spheres* mark the positions of bound anions.

3). The mutant exhibits a far-UV CD absorbance spectrum that is characteristic of a mixed α/β protein and is similar to the wild type, indicating that the overall fold of the M1775R domain is maintained in solution at 20 °C. BRCT-M1775R, however, is less stable, having a midpoint of thermal denaturation of ~41 °C, 11 °C less than the wild type protein (see Fig. 3, *inset* and "Experimental Procedures"). Consistent with these findings, solvent denaturation measurements of the thermodynamic stability of the BRCT tandem domain indicates that M1775R destabilizes the BRCT fold by 5.0 kcal/mol at 20 °C (36). Taken together, these results suggest that functional defects associated with BRCA1-M1775R may be attributed to destabilization of the BRCT domain at physiological temperatures.

X-ray Structure of Missense Variant M1775R—To gain structural insights into the destabilizing effect of M1775R, we crystallized and determined the structure of BRCT-M1775R at 2.8 Å (see Fig. 4*A*, Table I, and "Experimental Procedures"). $2F_o-F_c$ and F_o-F_c difference electron density indicate that structural rearrangements in response to the mutation are confined to residues within an ~5 Å radius of Arg-1775. Paired 4σ-positive and -negative electron density features in the F_o-F_c map near residue 1775 reveal that the substituted arginine is displaced from the hydrophobic core of the protein (Fig. 4*A*). The mutation is further accommodated by an ~1 Å shift of a neighboring residue, Pro-1776, in the $\beta1'$-$\alpha1'$ connecting loop and a series of side chain rearrangements that perturb the native inter-BRCT hydrogen bonding and van der Waals contact networks (Fig. 5, *A–C*).

Introduction of an arginine at position 1775 creates a clustering of three positively charged residues, Arg-1699, -1775, and -1835. In the native structure, Arg-1699 from the amino-terminal BRCT repeat participates in the sole conserved inter-BRCT repeat salt bridge with a pair of carboxyl-terminal BRCT acidic residues, Asp-1840 and Glu-1836 (Fig. 5*A*). Arg-1835 in human BRCA1 normally participates in a hydrogen bonding network with Gln-1811, thereby helping to orient the $\beta1'$-$\alpha1'$ loop (Fig. 5*A*). The positively charged guanidinium group of variant Arg-1775 is found positioned between two large positive peaks in our electron density maps that we have interpreted to be sulfate molecules, the highest concentration anion in the crystallization mother liquor (Figs. 4 and 5*B*). In the mutant, Arg-1699 retains the salt bridge with Asp-1840 but no longer contacts Glu-1836 and instead coordinates an anion. Arg-1835 rotates away from Gln-1811 and forms a new salt bridge with Glu-1836. Thus, it appears that electrostatic stabilization of this positive charge cluster is achieved through ordering of solvent anions and a cascade of hydrogen bonding alterations.

The adjustments in the positions of Arg-1775 and -1835 described above result in the displacement of the aliphatic portions of these side chains from the protein core (Fig. 5*C*). In response to these movements, Leu-1780 shifts to maintain van der Waals contact with the arginine residues. These movements are accomplished without the creation of large, energetically costly cavities within the hydrophobic core (33–35). The repacking of the core, however, in combination with instability created by hydrogen bonding changes and charge-charge repulsion of basic residues at the BRCT-BRCT interface may collectively help account for the 5 kcal/mol destabilization reported for the BRCT-M1775R protein (36).

Few crystallographic examples documenting protein structural responses to the introduction of charged residues into the hydrophobic core are available. Structural investigation of a comparable, highly destabilizing mutation in T4 lysozyme, Met-102 → Lys-102, reveals the position of the lysine side chain changes little when compared with native Met-102 packing (37). Instead, the mutation is accompanied by increased mobility of flanking residues, including a helix that normally packs against the substituted methionine. This motion allows access of the buried, basic side chain to solvent via a folding-unfolding transition of neighboring structured regions. The structural rearrangement that we observe in BRCT-M1775R is less dramatic but nevertheless results in the expulsion of the charged side chain from the hydrophobic protein core.

Destabilization of the BRCT Abrogates BRCA1-M1775R Function—At the surface of the protein, a hydrophobic groove near Met-1775 is apparent in the wild type structure (Fig. 5*D*). With the movement of Arg-1775 in the mutant, this cleft becomes occluded with charged atoms (Fig. 5*E*). This raises the possibility that, in addition to the destabilizing effect of the mutation, the substitution may disrupt association of BRCA1 with its interaction partners by directly modifying an exposed protein binding site. However, this site does not overlap with a BACH1 binding site that maps to the $\beta3$-$\alpha2$ connecting loop (Fig. 1) of the amino-terminal BRCT repeat (14), which is greater than 20 Å away from Met-1775. BACH1 binding is impaired by the M1775R substitution, suggesting that global structural defects resulting from the mutation, rather than localized structural and electrostatic perturbation, are responsible for the binding defect. Moreover, variant M1775R is defective in many biochemical assays that assess BRCA1 function and is unable to interact with several other proteins that associate with the wild type BRCT domain (Table II). It is unlikely that all of these proteins target a common surface near Met-1775 that is changed by the mutation. We therefore suggest that the wide spectrum of molecular defects reported for variant M1775R is explained by the destabilization of the domain.

Measurement of the steady state levels of BRCA1 missense variants M1775R, P1749R, and A1708E reveals they are similar to the wild type, suggesting that these proteins are not destabilized to the degree that they are degraded significantly *in vivo* (17, 23). Although it is difficult to predict individual energetic contributions of the M1775R rearrangements to BRCT destabilization, it is clear that the cumulative changes affecting the structure across the BRCT-BRCT interface result in a temperature-sensitive tandem BRCT domain (Figs. 2 and 3) that is defective in BRCA1 protein interaction, transcription, and DNA repair functions. In analogous studies, the quantitative measurement of the thermodynamic stability of the p53 tumor suppressor has shown that many of the common cancer-causing mutations are destabilizing. Consequently, p53 is inactivated by mutation, and cell cycle control is lost (38). Because many of the BRCT missense variants destabilize the BRCT to the same extent or more than M1775R (13, 36),[2] we might expect these variants to possess molecular and disease phenotypes similar to M1775R. Examination of the effects of other missense mutations on BRCA1 cellular function will be necessary to correlate BRCT loss of structure with BRCA1 loss of function and will further establish protein misfolding as a basic molecular mechanism of disease.

Acknowledgments—We thank Bob Luty for help with spectroscopy measurements, Jason S. Lamoureux and Brian L. Mark for assistance with x-ray data collection, and Youngchang Kim and the Structural Biology Centre 19-ID beamline staff for excellent technical support and discussion during synchrotron data collection.

REFERENCES

1. Miki, Y., Swensen, J., Shattuck-Eidens, D., Futreal, P. A., Harshman, K., Tavtigian, S., Liu, Q., Cochran, C., Bennett, L. M., Ding, W. *et. al.* (1994) *Science* **266,** 66–67

[2] R. S. Williams and J. N. M. Glover, manuscript in preparation.

2. Deng, C. X., and Brodie, S. G. (2000) *Bioessays* **22,** 728–737
3. Scully, R., and Livingston, D. M. (2000) *Nature* **408,** 429–432
4. Venkitaraman, A. R. (2002) *Cell* **108,** 171–182
5. Friedman, L. S., Ostermeyer, E. A., Szabo, C. I., Dowd, P., Lynch, E. D., Rowell, S. E., and King, M. C. (1994) *Nat. Genet.* **8,** 399–404
6. Futreal, P. A., Liu, Q., Shattuck-Eidens, D., Cochran, C., Harshman, K., Tavtigian, S., Bennett, L. M., Haugen-Strano, A., Swensen, J., Miki, Y. *et. al.* (1994) *Science* **266,** 120–122
7. Gayther, S. A., Warren, W., Mazoyer, S., Russell, P. A., Harrington, P. A., Chiano, M., Seal, S., Hamoudi, R., van Rensburg, E. J., Dunning, A. M. *et. al.* (1995) *Nat. Genet.* **11,** 428–433
8. Brzovic, P. S., Rajagopal, P., Hoyt, D. W., King, M. C., and Klevit, R. E. (2001) *Nat. Struct. Biol.* **8,** 833–837
9. Shen, D., and Vadgama, J. V. (1999) *Oncol. Res.* **11,** 63–69
10. Koonin, E. V., Altschul, S. F., and Bork, P. (1996) *Nat. Genet.* **13,** 266–268
11. Bork, P., Hofmann, K., Bucher, P., Neuwald, A. F., Altschul, S. F., and Koonin, E. V. (1997) *FASEB J.* **11,** 68–76
12. Callebaut, I., and Mornon, J. P. (1997) *FEBS Lett.* **400,** 25–30
13. Williams, R. S., Green, R., and Glover, J. N. M. (2001) *Nat. Struct. Biol.* **8,** 838–842
14. Joo, W. S., Jeffrey, P. D., Cantor, S. B., Finnin, M. S., Livingston, D. M., and Pavletich, N. P. (2002) *Genes Dev.* **16,** 583–593
15. Zhang, X., Morera, S., Bates, P. A., Whitehead, P. C., Coffer, A. I., Hainbucher, K., Nash, R. A., Sternberg, M. J., Lindahl, T., and Freemont, P. S. (1998) *EMBO J.* **17,** 6404–6411
16. Krishnan, V. V., Thornton, K. H., Thelen, M. P., and Cosman, M. (2001) *Biochemistry* **40,** 13158–13166
17. Scully, R., Ganesan, S., Vlasakova, K., Chen, J., Socolovsky, M., and Livingston, D. M. (1999) *Mol. Cell* **4,** 1093–1099
18. Monteiro, A. N., August, A., and Hanafusa, H. (1996) *Proc. Natl. Acad. Sci. U. S. A.* **93,** 13595–13599
19. Chapman, M. S., and Verma, I. M. (1996) *Nature* **382,** 678–679
20. Yarden, R. I., and Brody, L. C. (1999) *Proc. Natl. Acad. Sci. U. S. A.* **96,** 4983–4988
21. Cantor, S. B., Bell, D. W., Ganesan, S., Kass, E. M., Drapkin, R., Grossman, S., Wahrer, D. C., Sgroi, D. C., Lane, W. S., Haber, D. A., and Livingston, D. M. (2001) *Cell* **105,** 149–160
22. Li, S., Chen, P. L., Subramanian, T., Chinnadurai, G., Tomlinson, G., Osborne, C. K., Sharp, Z. D., and Lee, W. H. (1999) *J. Biol. Chem.* **274,** 11334–11338
23. Yu, X., Wu, L. C., Bowcock, A. M., Aronheim, A., and Baer, R. (1998) *J. Biol. Chem.* **273**. 25388–25392
24. Otwinowski, Z., and Minor, W. (1997) *Methods Enzymol.* **276,** 307–325
25. Brünger, A. T., Adams, P. D., Clore, G. M., DeLano, W. L., Gros, P., Grosse-Kunstleve, R. W., Jiang, J.-S., Kuszewski, J., Nilges, M., Pannu, N. S.,Read, R. J., Rice, L. M., Simonson, T., and Warren, G. L. (1998) *Acta Crystallogr. Sect. D Biol. Crystallogr.* **54,** 905–921
26. Jones, T. A., Zou, J. Y., Cowan, S. W., and Kjeldgaard (1991) *Acta Crystallogr. Sect. A* **47,** 110–119
27. Winn, M. D., Isupov, M. N., and Murshudov, G. N. (2001) *Acta Crystallogr. Sect. D Biol. Crystallogr.* **57,** 122–133
28. Collaborative Computational Project, Number 4 (1994) *Acta Crystallogr. Sect. D Biol. Crystallogr.* **50,** 760–763
29. Laskowski, R. A., MacArthur, M. W., and Thornton, J. M. (1998) *Curr. Opin. Struct. Biol.* **8,** 631–639
30. Esnouf, R. M. (1999) *Acta Crystallogr. Sect. D Biol. Crystallogr.* **55,** 938–940
31. Merritt, E. A., and Bacon, D. J. (1997) *Methods Enzymol.* **277,** 505–524
32. Nicholls, A., Sharp, K. A., and Honig, B. (1991) *Proteins* **11,** 281–296
33. Liang, J., Edelsbrunner, H., and Woodward, C. (1998) *Protein Sci.* **7,** 1884–1897
34. Eriksson, A. E., Baase, W. A., Zhang, X. J., Heinz, D. W., Blaber, M., Baldwin, E. P., and Matthews, B. W. (1992) *Science* **255,** 178–183
35. Matthews, B. W. (1996) *FASEB J.* **10,** 35–41
36. Ekblad, C. M., Wilkinson, H. R., Schymkowitz, J. W., Rousseau, F., Freund, S. M., and Itzhaki, L. S. (2002) *J. Mol. Biol.* **320,** 431–442
37. Dao-pin, S., Anderson, D. E., Baase, W. A., Dahlquist, F. W., and Matthews, B. W. (1991) *Biochemistry* **30,** 11521–11529
38. Bullock, A. N., and Fersht, A. R. (2001) *Nat. Rev. Cancer* **1,** 68–76